

CHAPTER FIVE

ENANTIOSELECTIVE OXIDATION OF D- AND L-GLUCOSE AT WELL-DEFINED METAL SURFACES

5.1. Introduction

The conditions thought necessary to observe enantioselective adsorption on single crystal surfaces were described by Gellman and co-workers [1]. They suggested that certain sites at kinked single crystal metal surfaces should be considered as being chiral provided the two steps constituting the kink site were of unequal length [1]. Reflection through a plane normal to such a surface produces a new surface which itself cannot be superimposed upon the original, and thus such kink sites should be chiral. Hence, chirality should be absent when surfaces contain steps of equal length on each side of the kink.

To examine this hypothesis concerning the intrinsic chirality of metal kink sites, a chiral probe is required. Gellman and co-workers [1] investigated the adsorption and desorption of 2-butanol on $\text{Ag}(643)^{\text{S}}$ and $\text{Ag}(643)^{\text{R}}$; in particular, they examined the difference in desorption enthalpies of R- and S-2-butanol using temperature-programmed desorption (TPD) [2]. The (643) plane may be written in microfacet notation [3], as $3(111)\times(310)$, i.e., a three atom wide (111) terrace separated by zigzag (310) steps. Unfortunately, within the precision of their experimental technique, no enantioselectivity could be detected in the desorption of (R-) or (S)-2-butanol from either $\text{Ag}(643)^{\text{R}}$ or $\text{Ag}(643)^{\text{S}}$ (i.e. there was no measurable difference in desorption enthalpies to within $\pm 0.1 \text{ kcal mol}^{-1}$). In addition, no difference was observed in the decomposition kinetics of the enantiomeric alkoxides formed on preoxidised $\text{Ag}(643)^{\text{S}}$ and $\text{Ag}(643)^{\text{R}}$ surfaces.

Theoretical work by Sholl [4] confirmed that chiral discrimination between kink sites and asymmetric molecular centres should give rise to an enantiomeric response (enantiospecific energy difference).

In their original paper, Gellman et al. [1] proposed that a necessary and sufficient condition for observing chirality in single crystal substrates was to note whether the magnitudes of the step lengths comprising the kink sites were different. If they were, the surface would be chiral. Attard and co-workers [5,6] suggested that this interpretation was an approximation since it did not take into account the surface geometry of the individual Miller index planes

of the two steps the junction of which forms the kink site. According to Attard, all kink sites should be considered as being chiral, even when the two steps have equal lengths. A detailed analysis of the surface crystallography for f.c.c. systems reveals that all kinked surfaces are chiral, irrespective of the magnitude of step lengths comprising the kink, save for the meso forms such as “stepped” surfaces of the $n(110)\times(100)$ or $n(100)\times(110)$ type.

In the present work the low reactivity Ag substrate used by Gellman has been replaced by the more reactive surface of platinum, and glucose, a relatively large probe molecule containing five chiral centres, has been used instead of 2-butanol. It was hoped that these modifications would enhance the likelihood of an enantioselective interaction.

Electrochemical investigations of glucose oxidation using polycrystalline electrodes have been described [7-12] and have been extended to include surfaces of well-defined crystalline structure [13-16]. The structure-sensitive nature of glucose oxidation has been confirmed [13-16], particularly in relation to the dependence of oxidation rate on terrace width.

From an electrochemical standpoint, D-glucose ($\text{HCO}-(\text{CHOH})_4-\text{CH}_2\text{OH}$) is not the chiral probe of choice because of the complexity of its electro-oxidation in aqueous solutions [13,16,17]. Glucose oxidation leads to the production of gluconolactone, gluconic and glucaric acids [18]. However, CO is also produced at the beginning of the electro-oxidation which is adsorbed strongly on platinum and blocks surface sites. Thus, a surface poison is produced which inhibits glucose reactions (i.e. all electrolytic activity is quenched [15,16]). This occurs in the potential range in which glucose is normally electro-oxidised, and this CO can only be removed at more positive overpotentials.

The principal advantages of D-glucose as a chiral probe are that it is not expensive and can be obtained in a very pure form. Furthermore, its enantiomer, L-glucose, although not cheap, is commercially available. Glucose gives rise to a strongly surface-sensitive electrochemical oxidation current at platinum single crystal electrodes [16].

Structure-sensitive reactions involve adsorption. Thus, if the initial step in D-glucose electro-oxidation is chemisorption onto the electrode surface, then the energetics of this adsorption step may be influenced by the “handedness” of any chiral kink sites present in the surface and this should be detectable by following changes in the electro-oxidation current.

Since glucose undergoes mutarotation in aqueous solutions (see Chapter One) [19], one should always prepare such solutions at least 12 hours prior to any electrochemical measurement to allow time for equilibrium to be reached.

Furthermore, the rates of all these reactions depend on surface structure, and also on anion adsorption, the dependencies being different for each type of surface site [16].

In addition to these structural aspects of glucose oxidation, it should be remembered that electrochemical oxidation of organic molecules in general has been intensively studied because the current generated in a fuel cell may be related to the amount of electroactive species present. Hence, a fuel-cell-based sensor incorporating chiral discrimination would have profound implications for electroanalysis and electrosynthesis.

The aim of the study presented in this chapter is to illustrate how the electrochemical surface science approach was used to demonstrate, for the first time, the intrinsic chirality of certain types of clean metal single crystal surfaces and their surface modified bi-metallic analogues.

5.2. Results

5.2.1. Electro-oxidation of D- and L-glucose on clean Pt chiral crystals

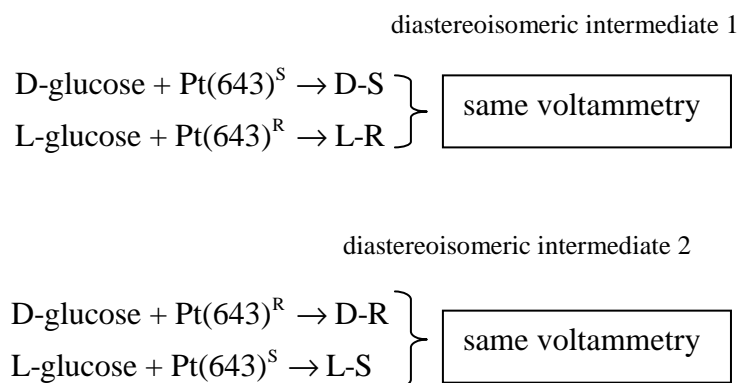
5.2.1.1. Pt(643)^R and Pt(643)^S

Fig. 5.1 illustrates the voltammetric response of Pt(643) electrode in contact with 0.1 M sulphuric acid. Three adsorption peaks are identified. The broad peak between 0.35 and 0.7 V is assigned to ionic adsorption from solution onto (111) terraces. The narrower, more intense peak at 0.22 V is associated with n(111)×(100) step sites [20]. Hence, the presence of (100) adsorption sites on Pt(643) is confirmed. Similarly, the peak at 0.06 V has been demonstrated to be characteristic of (111)×(111) or “110” sites [21]. Therefore, all of the adsorption sites predicted to be present on unreconstructed Pt(643) surface are observed experimentally. Furthermore, since the area under each peak should reflect the surface concentration of that particular type of site, the CV in Fig. 5.1 is entirely consistent with unreconstructed Pt(643).

In contrast to the behaviour at achiral surfaces (see Chapter One), when glucose electro-oxidation was repeated using (chiral) Pt(643)^R and Pt(643)^S electrodes, a clear enantiomeric response was obtained dependent on the stereochemical configuration of the glucose molecules (Fig. 5.2). Thus, D-glucose electro-oxidation on Pt(643)^S was observed to be identical to L-glucose electro-oxidation on Pt(643)^R, and, L-glucose electro-oxidation on Pt(643)^S was indistinguishable from D-glucose electro-oxidation on Pt(643)^R. Since the concentration of D- and L-glucose was 5 mM in all cases, the difference in voltammetry

represents chiral discrimination associated with the symmetry (R or S) of the surface. A true chiral recognition occurred in respect of the interaction between chiral adsorbate and chiral adsorbent.

A classical diastereomeric result involving two stereogenic centres was obtained and this constituted the first experimental confirmation of the intrinsic chirality of kinked metal single crystals.



A more detailed inspection of Fig. 5.2 reveals that, for the pair [D-glucose/Pt(643)^S + L-glucose/Pt(643)^R] (Fig. 5.2 (c) and (b)), the peak at 0.33 V (reaction at (111) terraces) is larger than the peak at 0.22 V (reaction at (111)×(100) steps), whereas the reverse is true for the alternative pairing of chiral surface and glucose [D-glucose/Pt(643)^R + L-glucose/Pt(643)^S] (Fig. 5.2 (a) and (d)). Interestingly, only a small amount of glucose decomposition (as measured by the magnitude of the current density at 0.07 V) takes place at the (110) step site of the kink. In fact, the oxidation peak at 0.33 V ((111) terraces) appears to be blocked on the first sweep for L-glucose oxidation on Pt(643)^S. Hence, we conclude that the Pt(643)^S electrode possesses a greater reactivity toward L-glucose as compared with D-glucose, and this is associated with the Pt(643)^S surface being chiral. In contrast, for Pt(643)^R, it is now D-glucose which gives rise to the greatest interaction with the (111) terrace sites, as signified by the absence of the peak at 0.33 V. The L-glucose adsorption peak at 0.33 V is clearly visible using Pt(643)^R.

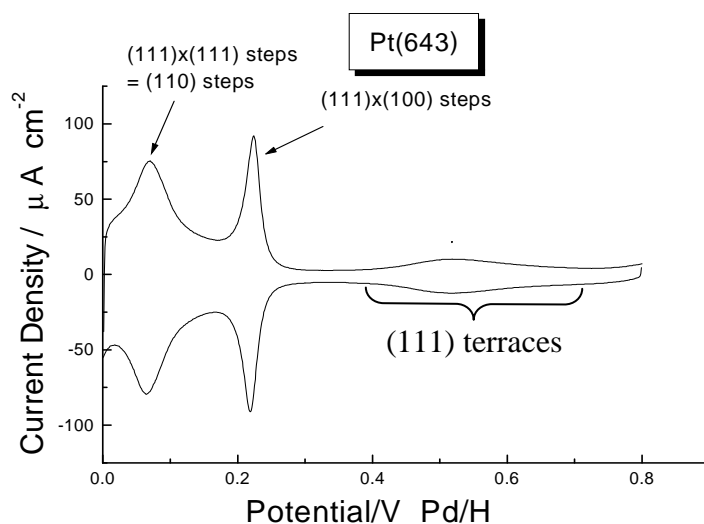


Fig. 5.1. Cyclic voltammogram of Pt(643)^R and Pt(643)^S in 0.1 M H₂SO₄ at sweep rate 50 mVs⁻¹.

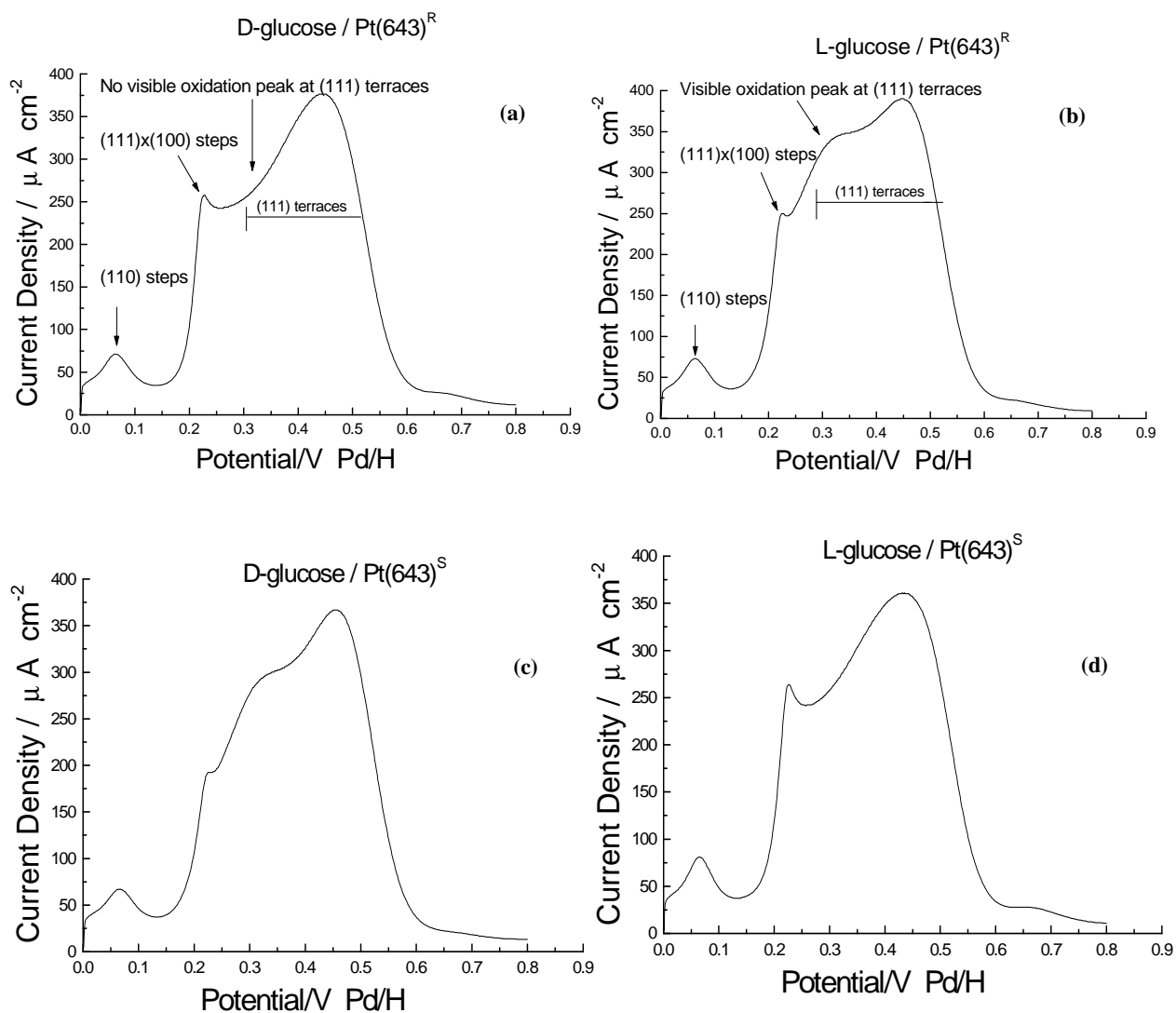
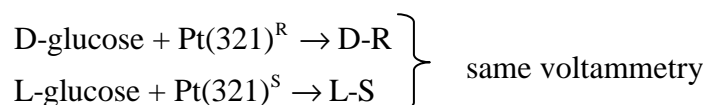
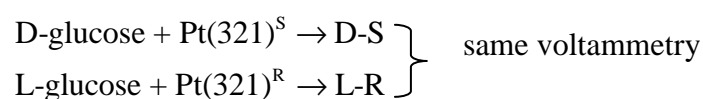


Fig. 5.2. LSVs for the electro-oxidation of 5 mM glucose on Pt(643) in 0.1 M H₂SO₄ at sweep rate 50 mV s⁻¹: (a) D-glucose/Pt(643)^R; (b) L-glucose/Pt(643)^R; (c) D-glucose/Pt(643)^S; (d) L-glucose/Pt(643)^S.

5.2.1.2. Pt(321)^R and Pt(321)^S

All steps in the Pt(321) surface are two atoms long and according to Gellman's discussion of kink sites, this surface should not give rise to an enantioselective response with glucose [1] because of the identical length of both steps.

Fig. 5.3 shows that electro-oxidation of glucose on this surface does in fact give an enantioselective response. A diastereomeric outcome similar to that observed with Pt(643) was observed:



These results show that the length of the two steps constituting the kink site is not the characteristic that determines the "handedness" of the kink, as originally proposed in reference [1]. Indeed, the magnitude of the enantioselective response (as measured by the difference in electric current density for R- and S- crystals) of the feature close to 0.3 V is found to be greater than for Pt(643).

5.2.1.3. Pt(531)^R and Pt(531)^S

Fig. 5.4 shows the electrode-oxidation of D- and L-glucose at Pt(531)^R and Pt(531)^S surfaces. This surface is unusual in that it is composed entirely of kink sites and contains no terraces or linear steps. This surface should not be chiral according to reference [1].

However, it is clear from Fig. 5.4 that very pronounced chiral discrimination occurred, as signified by the difference in rates of electro-oxidation at 0.31 V (the enantioselectivity is found to be still greater).

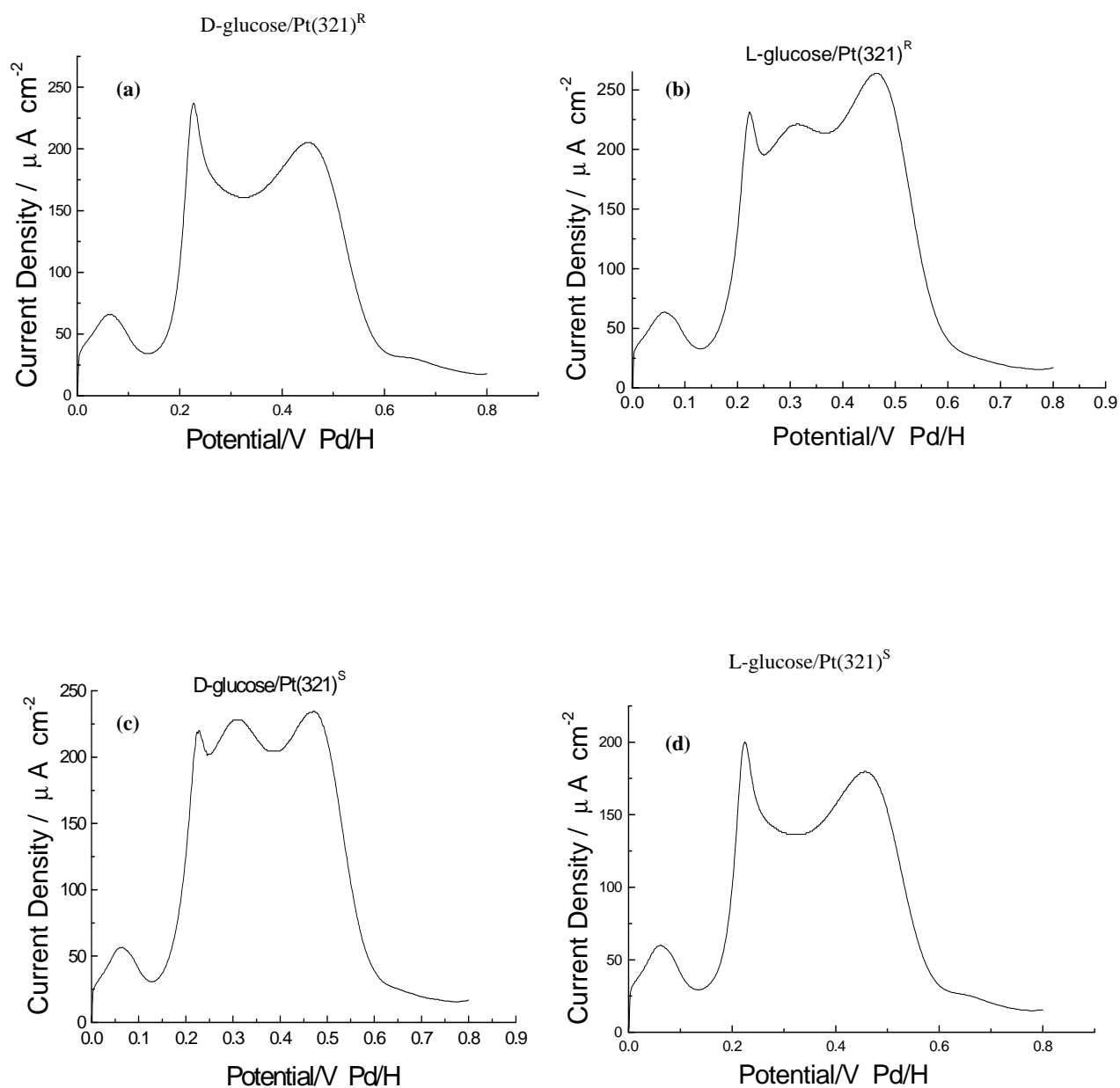


Fig. 5.3. LSVs for the electro-oxidation of 5 mM glucose on Pt(321) in 0.1 M H₂SO₄ at sweep rate 50 mV s⁻¹: (a) D-glucose/Pt(321)^R; (b) L-glucose/Pt(321)^R; (c) D-glucose/Pt(321)^S; (d) L-glucose/Pt(321)^S.

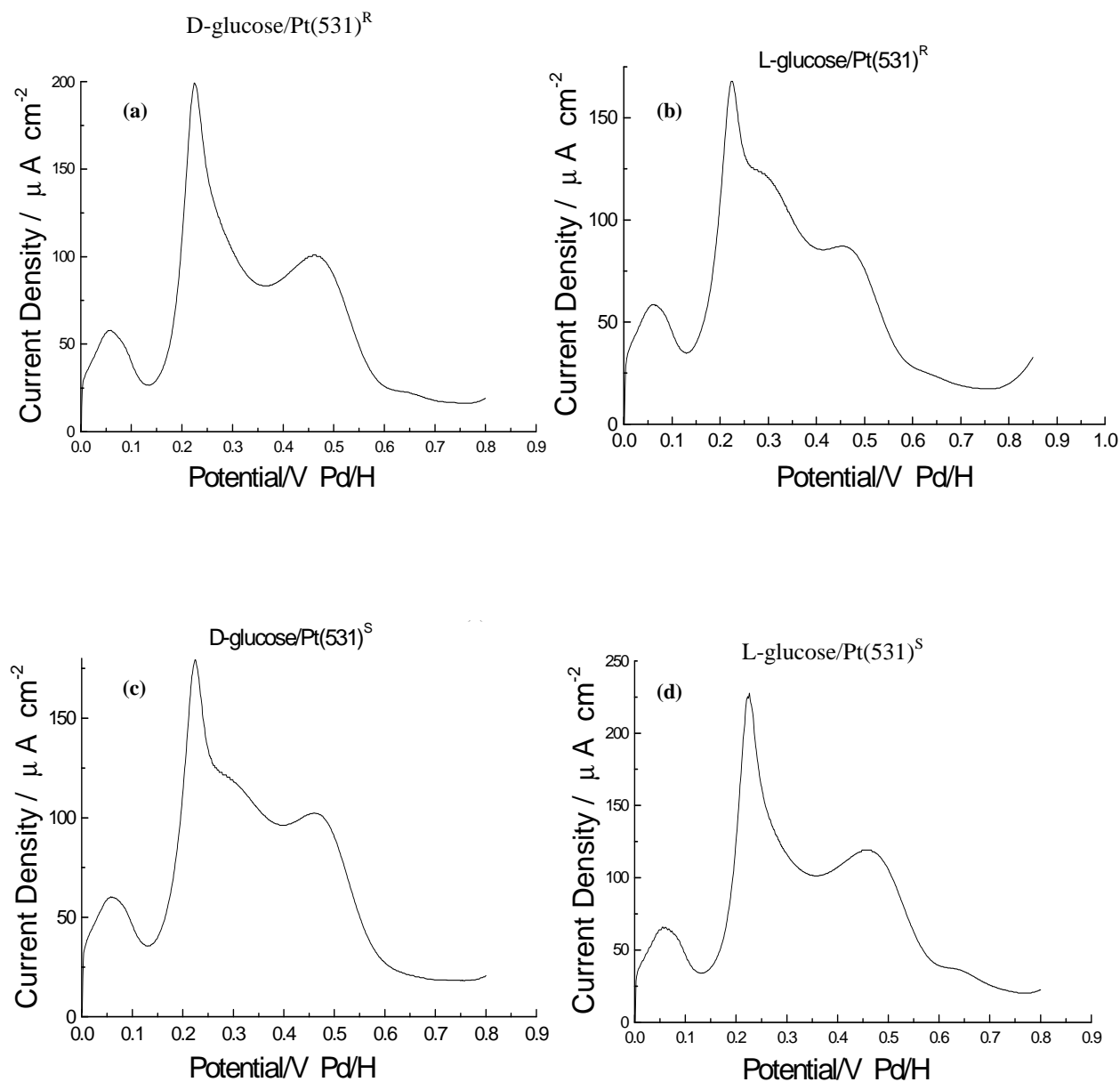


Fig. 5.4. LSVs for the electro-oxidation of 5 mM glucose on Pt(531) in 0.1 M H₂SO₄ at sweep rate 50 mV s⁻¹: (a) D-glucose/Pt(531)^R; (b) L-glucose/Pt(531)^R; (c) D-glucose/Pt(531)^S; (d) L-glucose/Pt(531)^S.

5.2.1.4. Pt(976)^R and Pt(976)^S

Fig. 5.6 shows the LSVs of electro-oxidation of D- and L-glucose on Pt(976)^R and Pt(976)^S. In this system it is hard to see any enantioselective response. This can be attributed to the fact that the kink density in this surface is lower than that at Pt(643), Pt(321) and Pt(531).

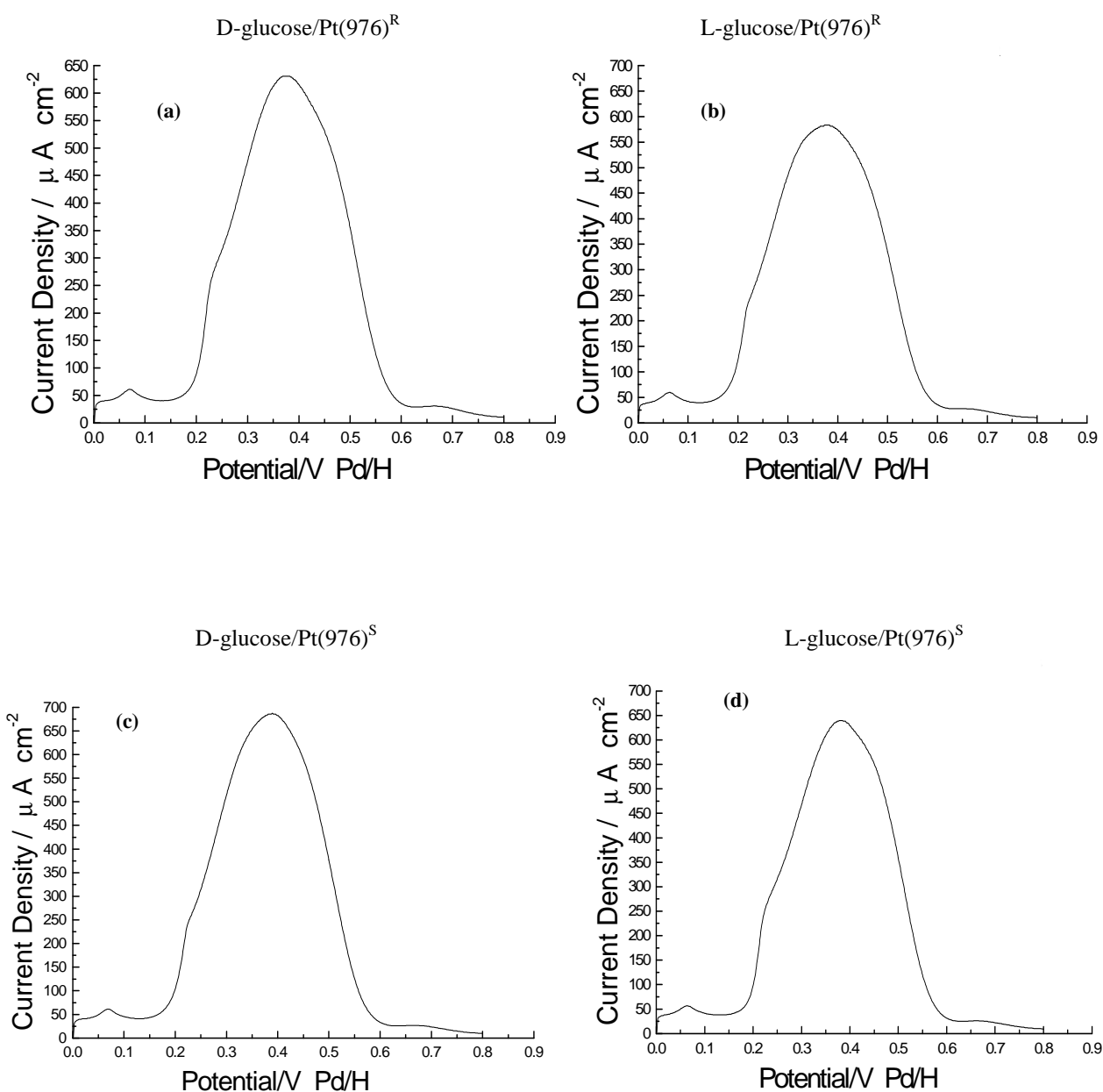


Fig. 5.6. LSVs for the electro-oxidation of 5 mM glucose on Pt(531) in 0.1 M H₂SO₄ at sweep rate 50 mV s⁻¹: (a) D-glucose/Pt(976)^R; (b) L-glucose/Pt(976)^R; (c) D-glucose/Pt(976)^S; (d) L-glucose/Pt(976)^S.

Calculations of enantioselective response

Electrochemical enantioselectivity is defined as the ratio of the difference in electro-oxidation (reaction rates) over their sum for a given R and S surface at a fixed potential V [22]:

$$S \% = \frac{(I_{R(v)} - I_{S(v)}) \times 100}{(I_{R(v)} + I_{S(v)})}$$

The structural sensitivity of glucose electro-oxidation may be seen when the surface density of kink sites is varied. This is exemplified in Fig. 5.5, where it can be seen that an increase in the surface density of kink sites on going from (643) to (321) leads to a greater degree of electro-oxidation enantioselectivity in the glucose reaction. For reaction at (111) terrace sites (at 0.38 V) $S(\text{Pt}(643)) < S(\text{Pt}(321)) < S(\text{Pt}(531))^1$, the absolute magnitude of the observed electric currents decreased on going from the less kinked to the most kinked surface (see Fig. 5.5). This is in accordance with expectation because the oxidation rate is known to increase markedly with increasing terrace width [13, 17].

Pt(531) entirely kinked surface - Pt(321) (2 atoms wide) - Pt(643) (3 atoms wide) - Pt(976) (6 atoms wide)

Nevertheless, for glucose electro-oxidation, the electrochemical enantioselectivity, S varies directly with the surface density of kink sites. These calculations show that chiral discrimination increases with the surface density of kink sites. This finding has important implications for heterogeneous catalysis. Supported metal catalysts contain a large number of

¹ For example: Oxidation current at 0.38 V for: D-glucose/Pt(643)^R = 333 μ A cm⁻², D-glucose/Pt(643)^S = 308 μ A cm⁻², D-glucose/Pt(321)^R = 180 μ A cm⁻², D-glucose/Pt(321)^S = 205 μ A cm⁻², D-glucose/Pt(531)^R = 80 μ A cm⁻², D-glucose/Pt(531)^S = 100 μ A cm⁻²

$$S_{D\text{-glucose}/Pt(643)} = \frac{(308 - 333) \times 100}{(308 + 333)} = 4\% , S_{D\text{-glucose}/Pt(321)} = \frac{(180 - 205) \times 100}{(180 + 205)} = 6.5\%$$

$$S_{D\text{-glucose}/Pt(531)} = \frac{(80 - 100) \times 100}{(80 + 100)} = 11\%$$

Hence the enantioselectivity reaction increases with moving from P(643) → Pt(321) → Pt(531), and this is due to the kink density on Pt(531) being higher than that on Pt(321) and Pt(643).

defect sites by virtue of their small particle size, although for polycrystalline materials, equal numbers of R and S type kinks are present at the surface. However, if a chiral promoter is adsorbed onto a polycrystalline substrate, it may be that kinks of a particular stereochemistry (R- or S-) will be favoured as adsorption sites compared to the enantiomorphic sites (S- or R). Enantioselective heterogeneous catalysis may then be achieved at enantiomorphic sites that remain free for catalysis [22].

It was reported by Attard and co-workers [22] that by using the values of current densities at 0.31 V, a diastereomeric excess of about 80 % was evaluated for glucose electro-oxidation on Pt(531). This compares with a value of 60% in the case of Pt(643). Inspection of our results in Fig. 5.5 indicates slight difference to Attard's previous findings.

In respect of glucose oxidation, clearly the (110) site plays a role in initially orienting the carbohydrate molecule in relation to the handedness of the kink, but the actual bond-breaking, surface reactions appear to proceed most readily at the (100) and (111) sites.

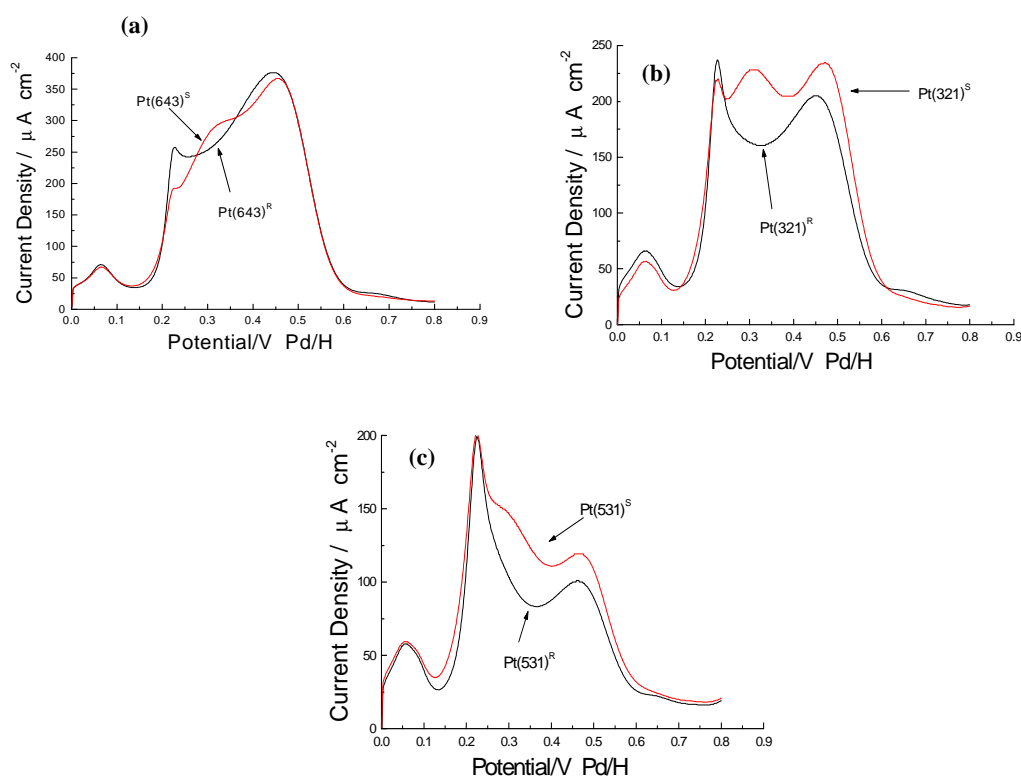


Fig. 5.5. Comparison of the linear sweep voltammograms (LSVs) for the electro-oxidation of 5 mM D-glucose in 0.1 M H₂SO₄ at sweep rate 50 mV s⁻¹: (a) Pt(643), (b) Pt(321), (c) Pt(531). Black curves represent behaviour at R-surfaces, coloured curves represent behaviour at S-surfaces.

5.3. Electro-oxidation of Glucose on Chiral Pt Surfaces Containing a Second Metallic Component

Deposition of Au, Ag and Bi on chiral Pt surfaces was presented in Chapter Four. In this work, the electro-oxidation of glucose was investigated on chiral surfaces partially or fully covered with Au, Ag, or Bi, in order to investigate the response of the enantioselectivity to the presence of these adatoms.

5.3.1. Au/Pt(321)

Fig. 5.7 illustrates the effect on the electro-oxidation LSVs of glucose of progressive subsequent deposition of Au. In the case of both Pt (321)^R and Pt(321)^S, the enantioselective response which was clear for the clean surfaces, disappears immediately after the addition of a small amount of Au (0.1 ML). The peak at about 0.33 V which was clear for the pair [D-glucose/Pt(321)^S + L-glucose/Pt(321)^R] disappears (Fig. 5.8 (b) and (c)). This modification of the glucose reaction leads to a reduction in the electrochemical enantioselectivity of glucose electro-oxidation which indicates that Au adatoms adsorb by blocking first the kink sites which are the junction between (100) and (110) steps in accordance with the results obtained in Chapter Four.

The activity for D- and L-glucose oxidation decreased as more and more Au was deposited on the Pt surface until no reaction occurred when 1 ML of Au had been formed (see the last LSVs in Figs. 5.7 (a), (b), (c) and (d)). This indicates that no enantiomeric interaction took place at the surface of the kinked Pt(321) electrode when it was covered partially or fully with Au.

When the pairs [D-glucose/Au/Pt(321)^S + L-glucose/Au/Pt(321)^R] and [D-glucose/Pt(321)^R + L-glucose/Pt(321)^S] are compared, it is clear that the effect of Au is the same for each pair, i.e. the enantioselective response which was so clear on pure Pt(321) is destroyed. Thus, as Au adatoms are deposited on these kinked surfaces, they become unable to distinguish between L- and D-glucose. This is interpreted to mean that kink sites which are responsible for the chiral recognition during D- and L-glucose adsorption and reaction on Pt(321)^R and Pt(321)^S become blocked by Au adatoms, and that these Au adatoms are not as active as the free Pt kink sites.

In fact, the oxidation peak at 0.33 V in the pair [D-glucose/Au/Pt(321)^S + L-glucose/Au/Pt(321)^R] is blocked first by Au adatoms, whereupon the system shows the same LSVs as the pair [D-glucose/Au/Pt(321)^R + L-glucose/Au/Pt(321)^S].

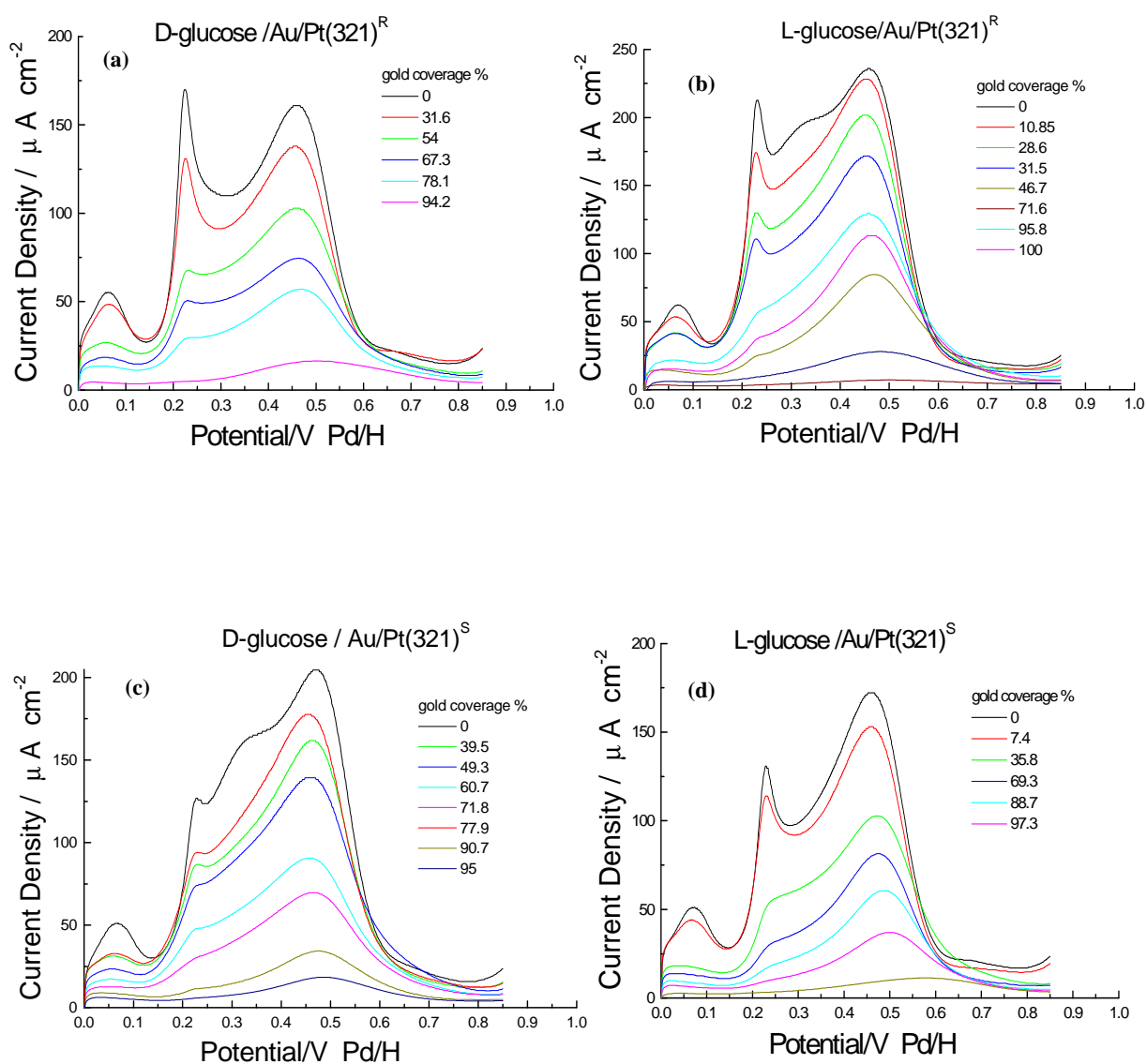


Fig. 5.7. LSVs for the electro-oxidation reaction of 5 mM glucose on Au-decorated Pt(321) in 0.1 M H_2SO_4 at sweep rate 50 mV s^{-1} : (a) D-glucose/Au/Pt(321)^R, (b) L-glucose/Au/Pt(321)^R, (c) D-glucose/Au/Pt(321)^S, (d) L-glucose/Au/Pt(321)^S.

5.3.2. Au/Pt(531)

Fig. 5.8 shows the electro-oxidation of D- and L-glucose on Pt(531) (which is composed entirely of kink sites) covered with Au. The first LSVs (black curves) represent the reaction on pure Pt(531)^R and Pt(531)^S. The behaviour of the pair [L-glucose/Pt(531)^R + D-glucose/Pt(531)^S] (black curves in Fig. 5.8 (b) and (c)) is identical. The oxidation peak at 0.30 V (111 terraces) appears already to be blocked on the first sweep for the pair [L-glucose/Pt(531)^S + D-glucose/Pt(531)^R] (black curves in Fig. 5.8 (a) and (d)). From this it is concluded that the Pt(531)^S electrode possesses a greater reactivity towards L-glucose as compared with D-glucose. Similarly, the Pt(531)^R electrode possesses a greater reactivity towards D-glucose as compared with L-glucose. This behaviour of glucose on this surface is like that on Pt(321)^R and Pt(321)^S.

When Au adatoms are added to this surface, it is clear that small concentrations of gold do not destroy the enantioselective response. Thus, this oxidation peak (at 0.30 V) can be seen clearly in the red curves and is just visible in the pair [D-glucose/Au/Pt(531)^S + L-glucose/Au/Pt(531)^R] (red curves in Figs. 5.8 (b) and (c)). However, as more Au was added to the surface, so the behaviour of glucose reaction became the same for both pairs [D-glucose/Au/Pt(531)^S + L-glucose/Au/(Pt(531)^R] and [D-glucose/Au/(Pt(531)^R + L-glucose/Au/Pt(531)^S]. The activity of the glucose reaction decreased in both cases until it stopped when the surface was fully blocked with Au. This finding further supports the view that a true enantiomeric interaction is taking place at the surface of the kinked platinum electrode when it is free of Au. For surfaces having a lower kink density (e.g. Pt(321)), small amounts of Au destroy the enantiomeric interaction (0.1 ML of Au (see Fig. 5.7 (b)), but for surfaces having a higher kink density or for those that consist entirely of kink sites, enantiomeric interactions persist to higher Au coverages (0.31 ML in the case of Pt(531) (see Fig. 5.8 (b)).

5.3.3. Ag/Pt(321)

Deposition of Ag on Pt(321)^R and Pt(321)^S was performed and then glucose oxidation investigated to determine the effect of the deposited Ag. Fig. 5.9 shows the electro-oxidation of D- and L-glucose on Pt(321)^R and Pt(321)^S. As in the case of Au/Pt(321), the rate of the glucose reaction decreased as Ag was added to the surface, but a clear enantiomeric response was retained. Indeed, D-glucose electro-oxidation on Pt(321)^S is identical to L-glucose electro-oxidation on Pt(321)^R, and, L-glucose reaction on Pt(321)^S is closely similar to that

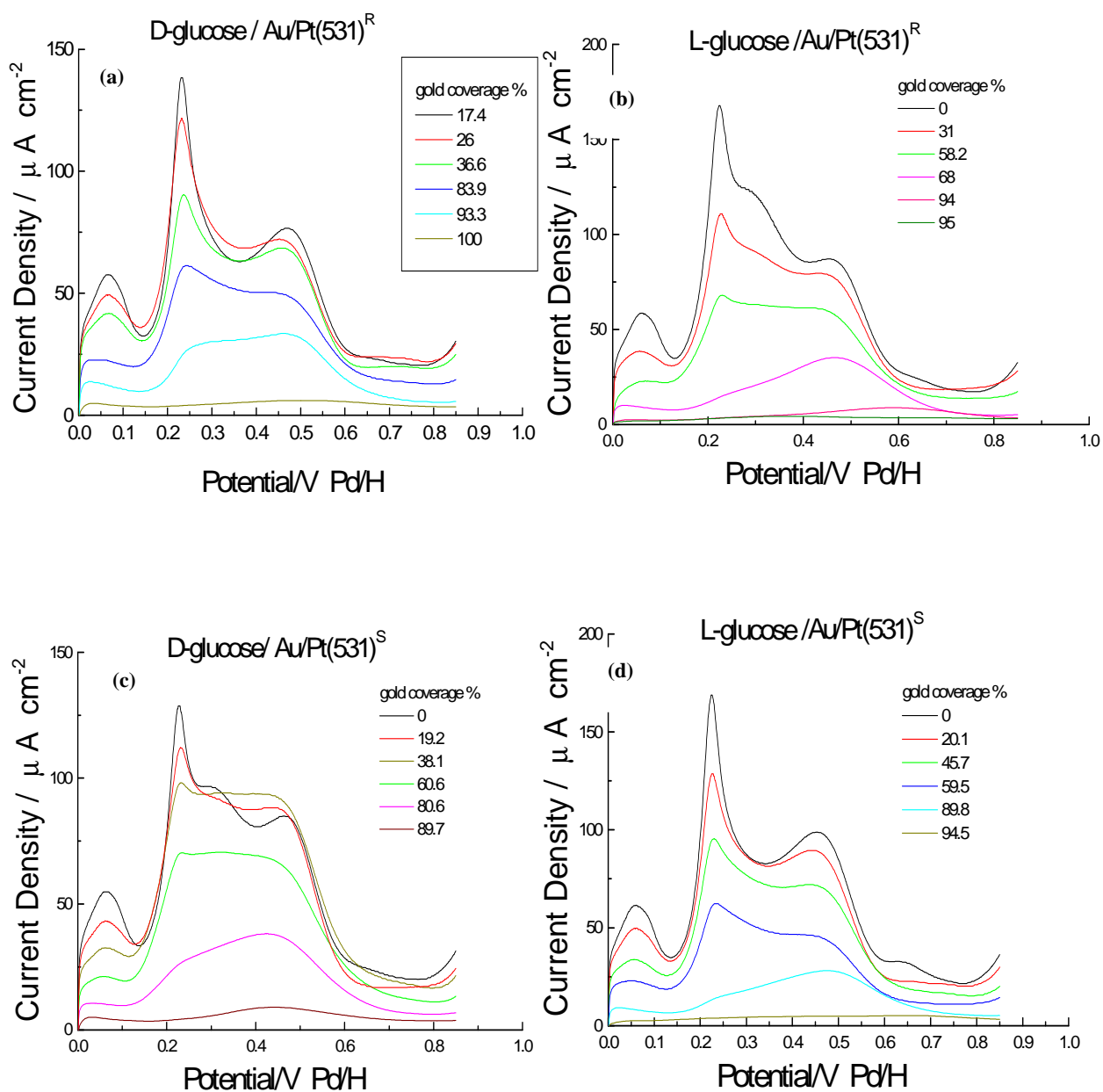
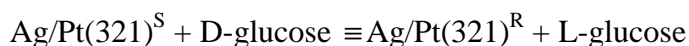


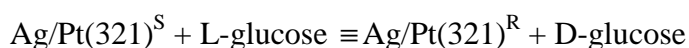
Fig. 5.8. LSVs for the electro-oxidation reaction of 5 mM glucose on Au-decorated Pt(531) in 0.1 M H₂SO₄ at sweep rate 50 mVs⁻¹.

- (a) D-glucose/Au/Pt(531)^R,
 (b) L-glucose/Au/Pt(531)^R,
 (c) D-glucose/Au/Pt(531)^S,
 (d) L-glucose/Au/Pt(531)^S.

of D-glucose reaction on Pt(321)^R. Since similar concentrations of Ag were added in each case, the voltammetric behaviour constitutes chiral discrimination. Hence, a classical diastereomeric result involving two stereogenic centres is realised, and this is the first determination of the intrinsic chirality of kinked metal single crystals covered with Ag. Thus:



and



The LSVs in Figs. 5.9 (b) and (c) are virtually identical. The oxidation peak at 0.33 V remained visible even after filling one-third of kink sites (0.07 ML of Ag (see Figs. 5.9 (b) and (c) green curves)). With more Ag added to the surface, total current densities representing overall oxidation decreased but the oxidation peak at 0.33 V remained visible whereas those at 0.2 V and 0.48 V disappeared (Figs. 9 (b) and (c)). A new oxidation peak became visible at 0.15 V when 0.075 ML of Ag was formed (one-third of the kink sites were filled (see the peak at 0.05 V ((110) sites)). This new peak reached a maximum current of 50 $\mu\text{A cm}^{-2}$ at 0.15 V, then it decreased in magnitude as more Ag was added until it disappeared when the surface was fully covered with Ag.

In the case of the pair [D-glucose/Ag/(321)^R + L-glucose/Ag/(321)^S], the LSVs in Figs.5.9 (a) and (d) are identical. The difference between the LSVs for this pair of reactions as compared to the other pair, is that the shape of the peak at 0.25 to 0.3 V is narrower, the LSVs are thinner, and do not have an oxidation peak at 0.15 V.

5.3.4. Ag/Pt(531)

The oxidation of D- and L-glucose on Pt(531)^R and Pt(531)^S decorated by various amounts of Ag was also investigated. From the LSVs in Fig. 5.10, it is clear that the pair [D-glucose/Ag/(531)^R + L-glucose/Ag/Pt(531)^S] show identical behaviour, as do the other pair [D-glucose/Ag/(531)^S + L-glucose/Ag/Pt(531)^R]. Both pairs behave similarly with respect to oxidation reaction activity, the activity decreasing as more Ag was added.

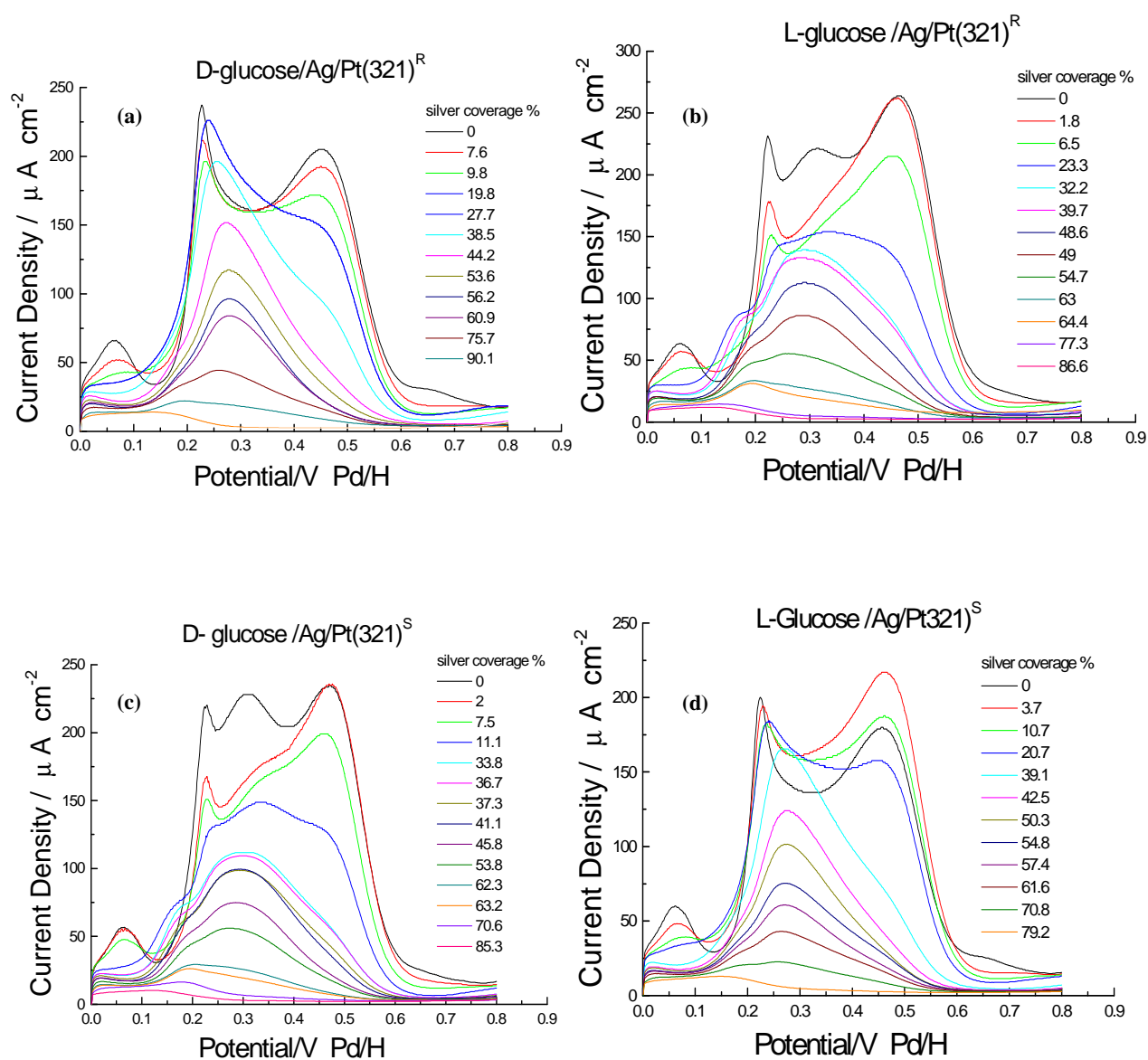


Fig. 5.9. LSVs for the electro-oxidation reaction of 5 mM glucose on Ag-decorated Pt(321) in 0.1 M H₂SO₄ at sweep rate 50 mV s⁻¹:

- (a) D-glucose/Ag/Pt(321)^R,
- (b) L-glucose/Ag/Pt(321)^R,
- (c) D-glucose/Ag/Pt(321)^S,
- (d) L-glucose/Ag/Pt(321)^S.

The oxidation peak at 0.33 V (Figs. 5.10 (b) and (c)) remained visible even after one-quarter of the kink sites were filled by Ag (0.07 ML formed (see Figs. 5.10 (b) and (c)-green curves), but, as more Ag was added, the LSVs became broader in shape, and an oxidation peak appeared at about 0.15 V when about three-quarters of the kink sites were filled (0.3 ML formed see blue curves in (b) and (c)). The intensity of this peak decreased as more Ag was added until it eventually disappeared when the kinks were almost filled with Ag. In the case of pair [D-glucose/Ag/Pt(531)^R + L-glucose/Ag/Pt(531)^S] (Figs. 5.10 (a) and (d)), the oxidation LSVs decrease in magnitude (electric currents) but there is no visible oxidation peak as in the case of pair [D-glucose/Ag/Pt(531)^S + and L-glucose/Ag/Pt(531)^R].

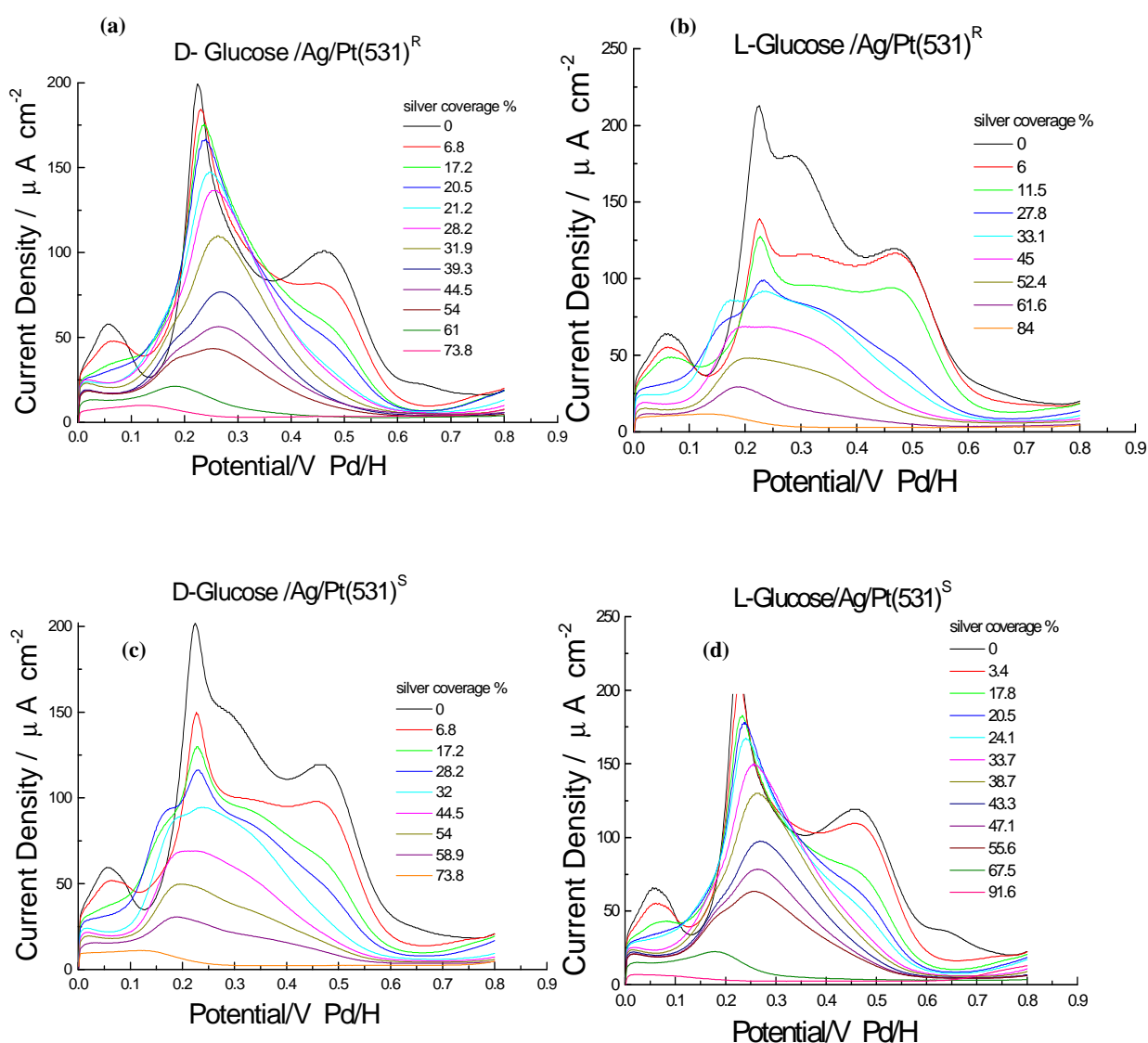


Fig. 5.10. LSVs for the electro-oxidation reaction of 5 mM glucose on Ag-decorated Pt(531) in 0.1 M H₂SO₄ at sweep rate 50 mV s⁻¹:

- (a) D-glucose/Ag/Pt(531)^R,
 (b) L-glucose/Ag/Pt(531)^R,
 (c) D-glucose/Ag/Pt(531)^S,
 (d) L-glucose/Ag/Pt(531)^S.

5.3.5. Ag/Pt(643)

Fig. 5.11 shows the electro-oxidation reaction on $\text{Pt}(643)^{\text{R}}$ and $\text{Pt}(643)^{\text{S}}$ as it was progressively covered with Ag. The activity for D- and L-glucose oxidation decreased as Ag was added to both surfaces. The oxidation peak at 0.33 V (in Fig. 5.11 (b) and (c)) was still visible even after filling one-half of the kink sites (0.25 ML of Ag, Figs. 5.11 (b) and (c) green lines). This peak became dominant as more Ag was added, and another oxidation peak became visible at 0.15 V, which disappeared when the kink sites were almost covered. This

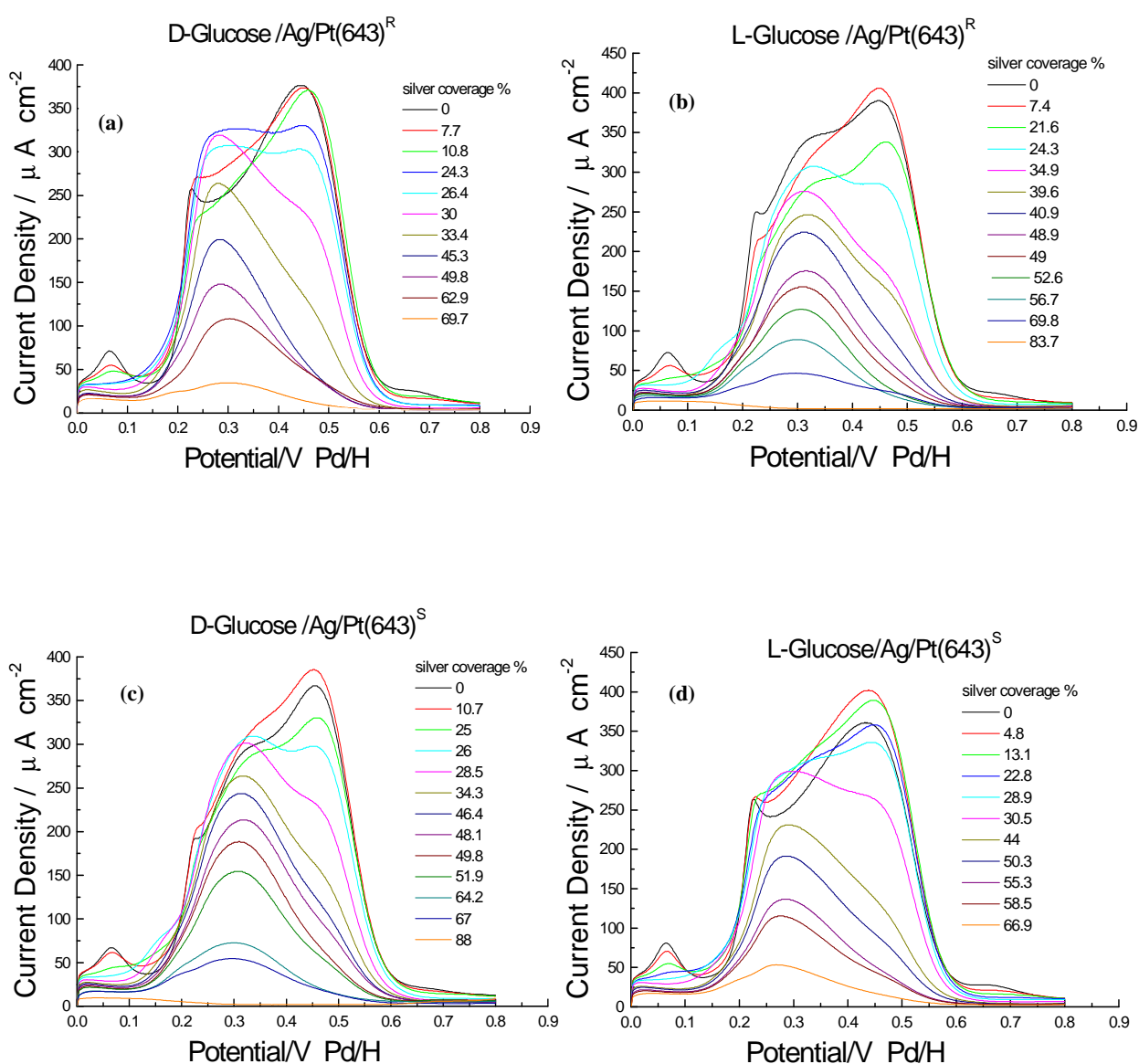


Fig. 5.11. LSVs for the electro-oxidation reaction of 5 mM glucose on Ag-decorated Pt(643) in 0.1 M H_2SO_4 at sweep rate 50 mV s^{-1} :

- (a) D-glucose/Ag/Pt(643)^R,
- (b) L-glucose/Ag/Pt(643)^R,
- (c) D-glucose/Ag/Pt(643)^S,
- (d) L-glucose/Ag/Pt(643)^S.

new peak was not seen for the reaction pair [D-glucose/Ag/Pt(643)^R + L-glucose/Ag/Pt(643)^S] (Fig. 5.11 (a) and (d)). The shape of the LSVs of glucose oxidation after the new oxidation peak disappears is similar for the pairs [D/R, L/S] and [D/S, L/R].

The enantioselective response for this surface is not as marked as that for Pt(321) and Pt(531) because the kink density is lower. This finding gives further support to the importance of kink sites in the electro-oxidation of glucose; for surfaces containing kinks, when the kinks are blocked the LSVs become indistinguishable.

5.3.6. Ag/Pt(976)

Fig. 5.12 illustrates the effect of adding Ag to the surface of Pt(976) on the oxidation of glucose. The enantioselective response of glucose reaction on clean Pt(976) (which has a lower kink density than the other surfaces) is slight as explained earlier (section 5.2.1.4). It is clear from Fig. 5.12 that adding Ag to this surface provides no new features. Activity decreases in the same way over both surfaces.

5.3.7. Bi/Pt(321)

Fig. 5.13 shows the LSVs for the electro-oxidation of glucose on Bi/Pt(321). For the reaction pair [L-glucose/Bi/Pt(321)^R + D-glucose/Bi/Pt(321)^S] (Figs. 5.13 (c) and (b)) it is evident that adding Bi to the surface increased the activity for glucose oxidation. The maximum current was reached when three-quarters of the kink sites were blocked by Bi (0.45 ML of Bi), and beyond this point the activity decreased (Figs. 5.13 (b), (c)). This behaviour can be seen in the reaction pair [D-glucose/Bi/Pt(321)^S + L-glucose/Bi/Pt(321)^R] as well (Figs. 5.13 (a), (d)). In Figs. 5.13 (c) and (b), the oxidation peak at 0.33 V remained visible until about one-half of the kink sites were filled (0.3 ML of Bi), but this peak disappeared when the activity started to decrease. At this point the LSVs for the reaction pair [D-glucose/Bi/Pt(321)^S + L-glucose/Bi/Pt(321)^R] (Figs. 5.13 (b) and (c)) became similar to those for the pair [D-glucose/Bi/Pt(321)^R + L-glucose/Bi/Pt(321)^S] (Fig. 5.13 (a) and (d)).

When the surface was completely blocked by Bi (see Figs. 5.13 (e) and (f)) glucose oxidation continued (see Figs. 5.13 (a) to (d), magenta curves) the enantioselective response no longer existed, the LSVs being indistinguishable from each other. Most noteworthy, however, was that for the D-/R- and L-/S- pairing, growth in the intensity of a peak at 0.3 V

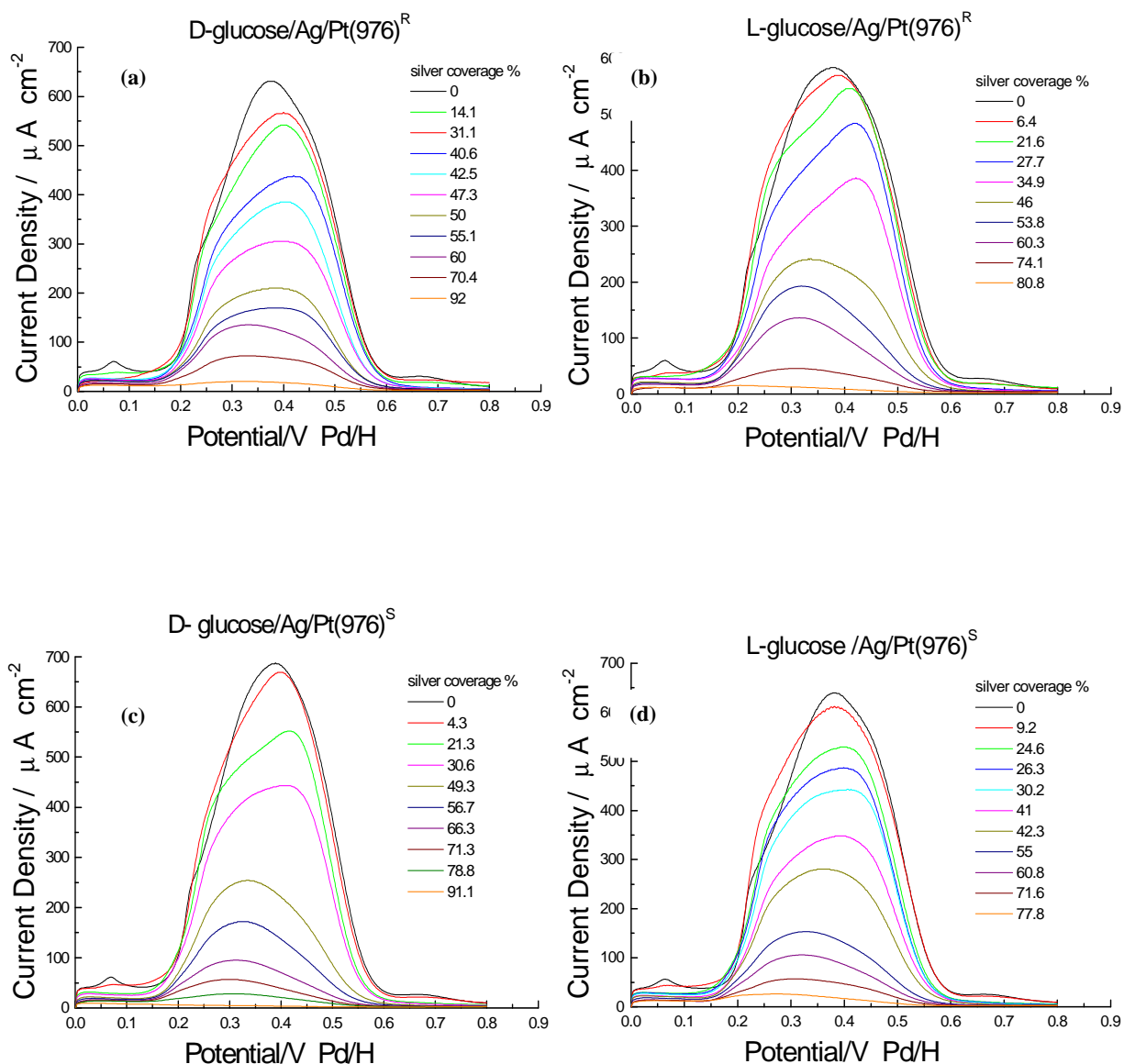


Fig. 5.12. LSVs for the electro-oxidation reaction of 5 mM glucose on Ag-decorated Pt(976) in 0.1 M H₂SO₄ at sweep rate 50 mV s⁻¹:
 (a) D-glucose/Ag/Pt(976)^R,
 (b) L-glucose/Ag/Pt(976)^R,
 (c) D-glucose/Ag/Pt(976)^S,
 (d) L-glucose/Ag/Pt(976)^S.

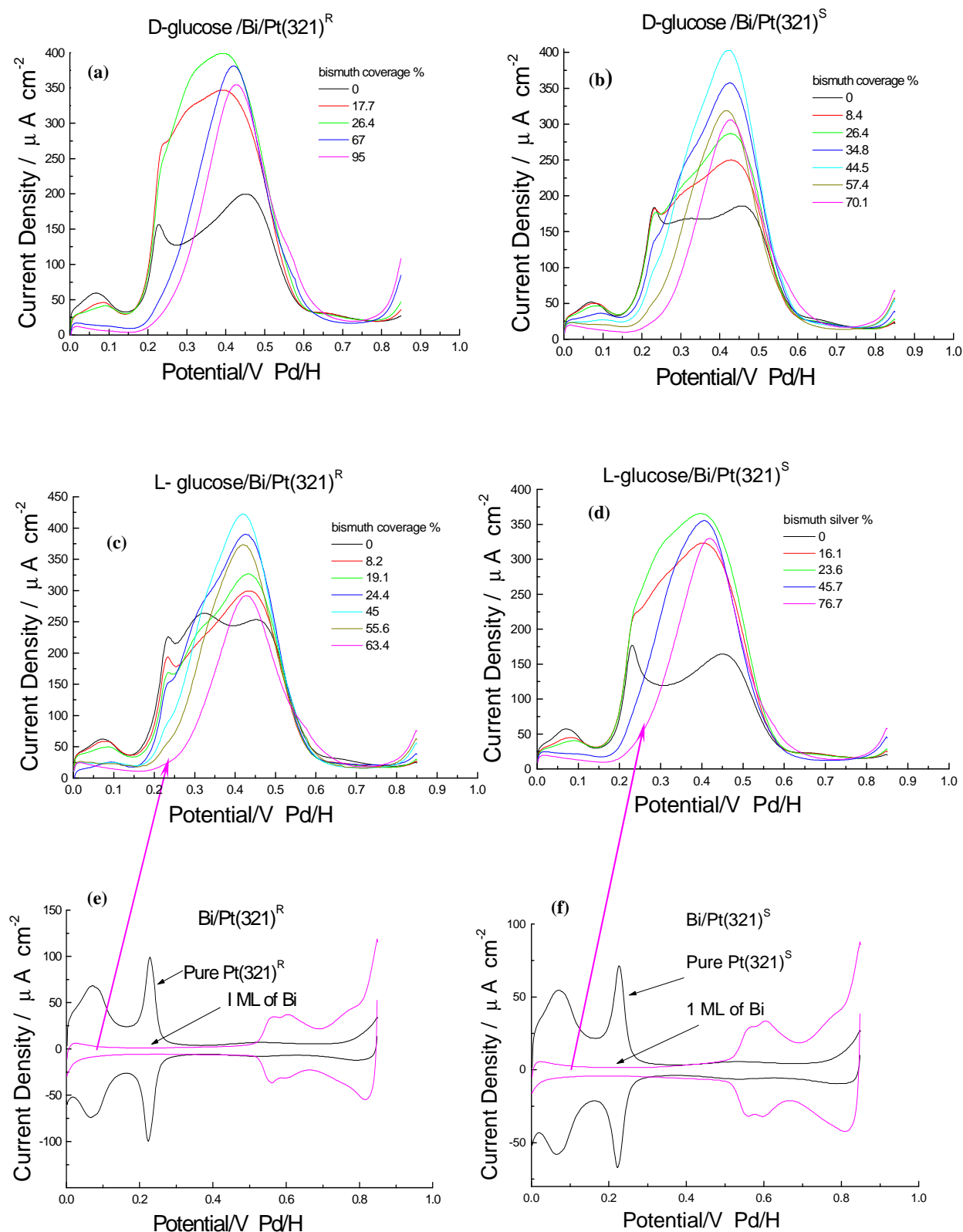


Fig. 5.13. LSVs for the electro-oxidation reaction of 5 mM glucose on Bi-decorated Pt(321) in 0.1 M H₂SO₄ at sweep rate of 50 mV s⁻¹: (a) D-glucose/Bi/Pt(321)^R, (b) D-glucose/Bi/Pt(321)^S, (c) L-glucose/Bi/Pt(321)^R, (d) L-glucose/Bi/Pt(321)^S, (e) CV for Pt(321)^R covered with \cong 1 ML of Bi, (f) CV for Pt(321)^S covered with \cong 1 ML of Bi.

is observed, i.e. at the same potential as the Bi-free surface chiral peak for the L-/R- and D-/S- combination. If this new peak corresponds to the same surface process, this means that when bismuth is adsorbed at defect sites, a switching in the sense of the chiral induction is occurring (indeed as, bismuth is added to the D-/S- and L-/R- systems, the 0.33 V peak is attenuated). It should be realised that this behaviour also coincides with the growth of a bismuth-induced clean surface peak at approximately the same potential (see Chapter Four) which was ascribed to sites at the “top” of the defect site. It would be an interesting observation to ascertain if the initial ‘attack’ of the glucose molecule (top or bottom of step) is dependent on whether or not bismuth is adsorbed at the defect site and hence leads to a dependence of chiral interaction on kink composition.

5.3.8. Bi/Pt(643)

Fig. 5.14 shows the electro-oxidation LSVs of D- and L-glucose on Bi/Pt(643). There is an enantioselective response between the reaction pairs [D-glucose/Bi/Pt(643)^R + L-glucose/Bi/Pt(643)^S] and [D-glucose/Bi/Pt(643)^S + L-glucose/Bi/Pt(643)^R]. This difference was retained until three-quarters of the kink sites were filled with Bi (0.5 ML of Bi) (Figs. 5.14 (c) and (b)). On reaching this point the oxidation peak which was observed for the reaction pair [D-glucose/Bi/Pt(643)^S + L-glucose/Bi/Pt(643)^R] at 0.33 V disappeared and the LSVs after this point were indistinguishable from those for the pair [D-glucose/Bi/Pt(643)^R + L-glucose/Bi/Pt(643)^S].

The LSVs in Figs. 5.14 (a), (b), (c) and (d) for the highest Bi loadings (magenta curves) represent the electro-oxidation of glucose when the Pt surface is completely blocked with Bi (see Figs. 5.14 (e) and (f)); these LSVs are similar in shape, demonstrating that the reaction is not enantioselective when the surface is completely blocked with Bi. This behaviour follows that observed over Pt(321)^R and Pt(321)^S. Again the production of a new glucose electro-oxidation peak at 0.3 V for the D-/R- and L-/S- combination should be noted when bismuth decorates defect sites.

5.3.9. Discussion and Conclusion

This investigation of the electro-oxidation of D- and L-glucose on pure chiral Pt single crystals not only provides experimental evidence for the intrinsic chirality of surface kinks, but also that chiral interaction may be modulated strongly by the presence of adatoms.

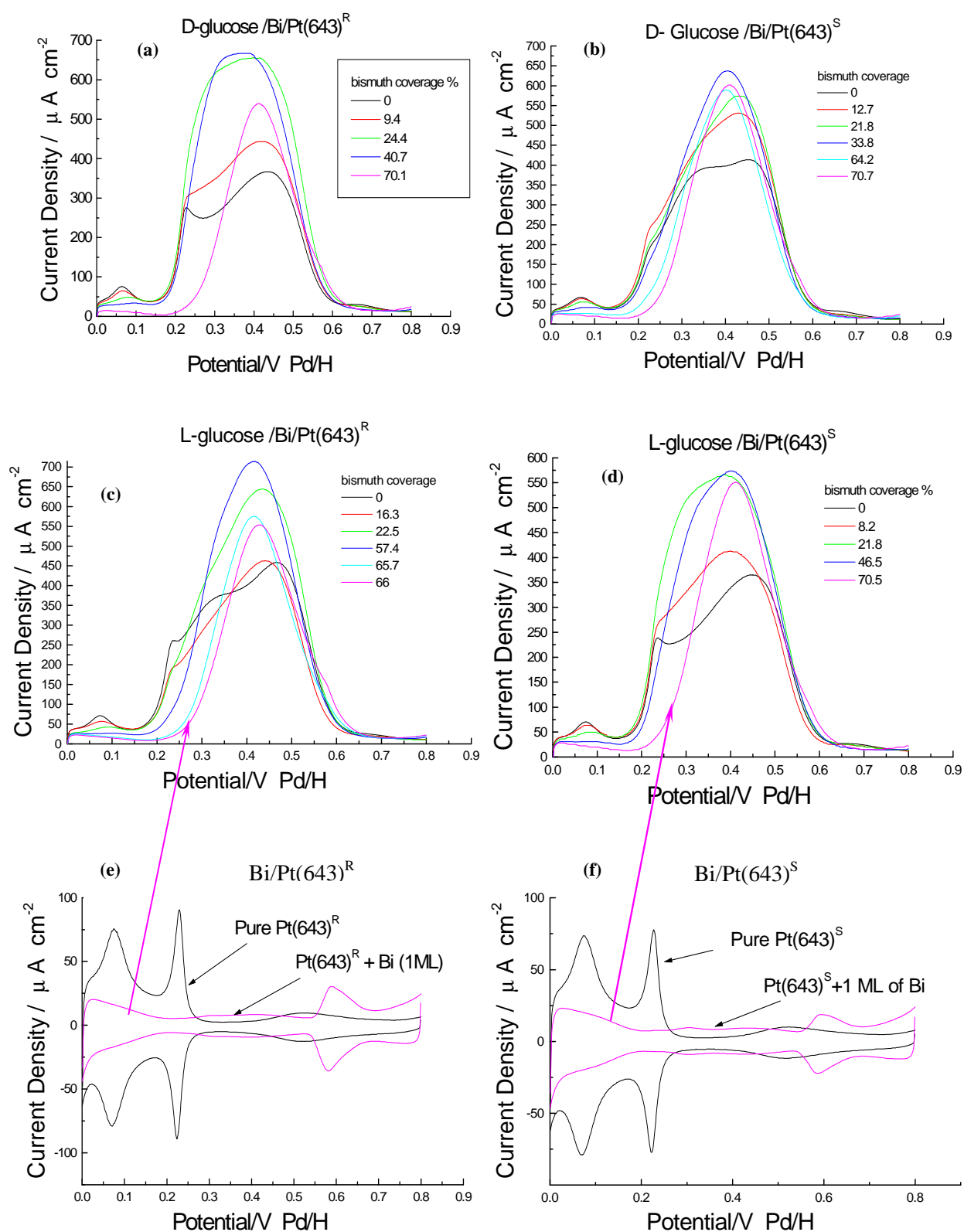


Fig. 5.14. LSVs for the electro-oxidation reaction of 5 mM glucose on Bi-decorated Pt(643) in 0.1 M H₂SO₄ at sweep rate of 50 mV s⁻¹: (a) D-glucose/Bi/Pt(643)^R, (b) D-glucose/Bi/Pt(643)^S, (c) L-glucose/Bi/Pt(643)^R, (d) L-glucose/Bi/Pt(643)^S, (e) CV for Pt(643)^R covered with \cong 1 ML of Bi. (f) CV for Pt(643)^S covered with \cong 1 ML of Bi.

Attard in a review [22] mentioned the results of electro-oxidation of a series of sugars which differed from each other in the handedness of a single carbon centre (see Fig. 5.15). These sugars, mannose, xylose and arabinose, were adsorbed onto a chiral kinked platinum electrode and the initial electro-oxidation current was monitored. The LSVs for these sugars have been reported in Chapter One Section 1.9.3.3. Although each sugar gives rise to its own singular response, a number of features are common to all LSVs, the most important being the absence or presence of a peak at 0.35 – 0.4 V (in this notation ‘peak A’) corresponding to reaction at (111) terraces. For D-glucose/R-kinks and L-glucose/S-kinks, peak A is not present whereas for D-glucose/S-kinks and L-glucose/R-kinks it is clearly discerned. Although the LSVs for mannose differ from those for glucose, once again the presence of peak A is observed for the D/S and L/R combinations, whereas it is not present for the D/R and L/S pairs. Glucose and mannose differ only in the chirality of the carbon atom at position 2. This suggests that changing the stereogenic centre at this position does not in itself alter the chiral relationship between the chemisorbate and the metal surface. In contrast, when D- and L-arabinose were investigated, it was found that peak A was present for the D/R combination but not present for the D/S. There are two differences between arabinose and glucose: the first is the change in chirality at carbon atom position 3, and the second is that arabinose does not contain a CH₂OH substituent at ring position 5. Either of these two features could mark out arabinose from glucose. However, when xylose was investigated (which like arabinose does not contain a CH₂OH group at position 5), the S/D and L/R combinations did give rise to peak A, just like glucose and mannose. Because xylose possesses the same chirality as glucose and mannose at position 3, whereas in arabinose the chirality is reversed, it has been suggested by Attard [22] that chiral discrimination between the glucose at carbon 3 and the kink gives rise to the enantioselective reaction associated with peak A. It is well-known that sugars undergo mutarotation in aqueous solution to produce the α and β forms (see Fig. 5.15) of pyranose and furanose (see Chapter One) [23]. For all sugars studied, the percentage of furanose in solution should be negligible. For the pyranose in aqueous solution, it was found that mannose and arabinose gave rise to 60% and 40%, whereas for xylose and glucose, the proportions were 64% and 36% [22]. Hence, speciation behaviour cannot account for the enantioselectivity displayed by the four sugars in relation to peak A. Combining this information with the seeming lack of reactivity of the (110) site and the knowledge from previous isotopic substitution experiments on glucose that initial C-H bond cleavage at carbon position 1 takes place on

Pt(111) [17], together with variation in *S* upon changing kink density and shape, it may be possible to begin modelling the interaction of chiral molecules with chiral kinks in a new fundamental manner. Fig. 5.16 shows an optimised structure for the D- and L-glucose on Pt(643)^S. The chiral centre at position 3 has been positioned as close to the chiral kink site as possible. In addition, the hydrogen-carbon bond at position one, which is known to dissociate during the glucose electro-oxidation reaction [17], has been directed toward the (111).

When a clean kinked surface was decorated with Au the enantioselective response of glucose disappeared as Au was added, the behaviour of D- and L-glucose became the same with decreasing oxidation activity until reaction completely stopped when the surface was fully covered with Au.

In the case of Ag, the enantioselective response remained visible until about three-quarters of the kink sites were filled; a new oxidation peak appeared at 0.15 V which disappeared as more Ag was added. This new peak was visible for the reaction pair [D/S + L/R] but not for the pair [D/R + L/S]. For both surfaces the activity for the glucose reaction decreased as more Ag was added; reaction stopped when the surface was completely filled with Ag.

The enantiomeric response shown by some R and S Ag/Pt surfaces, hopefully opens up the possibility of studying reactions of various organic molecules on chiral and achiral surfaces in order to refine some reaction mechanisms that are presently unclear or in dispute.

The electro-oxidation of D- and L-glucose was investigated on chiral Pt surfaces modified with Bi. It was hoped that enantiomeric response would be retained to very high coverages of Bi (because Bi activates some organic reactions when deposited on achiral surfaces (See Chapter Four, Section 4.1)); however, this was not the case.

All the above findings support the hypothesis that kink sites play a crucial role in these observed enantiomeric interactions at chiral surfaces. In addition, the different adsorption behaviour of Au, Ag and Bi (epitaxial monolayers formed, surface alloys formed and selective occupation of defect sites respectively) and their relation to surface chirality deserves further comment. The behaviour of Ag as a surface modifier is very reminiscent of chiral Pd-Pt bulk alloy prepared by Watson [24] in its interaction with glucose. In that work, the bulk alloy remained enantioselective with respect to glucose oxidation in spite of rather high palladium surface coverages. Such behaviour was not observed with palladium monolayers. This accords with the fact that the Ag-Pt surface alloys remain enantioselective to much higher metal loadings than, for example, gold, which simply blocks chiral kink sites.

Bismuth is special because not only does it enhance electrocatalytic activity, at least so long as terrace sites remain free, but it also appears to “switch” the sign of the chiral interaction. This is believed to be related to the induction of new electronic states at the terrace sites at the “top” of the kink edge. The approach of a three dimensional chiral object to a defect site from top or bottom should lead to a different enantioselective outcome as appears to be the case for Bi on chiral Pt surfaces vicinal to (111) planes.

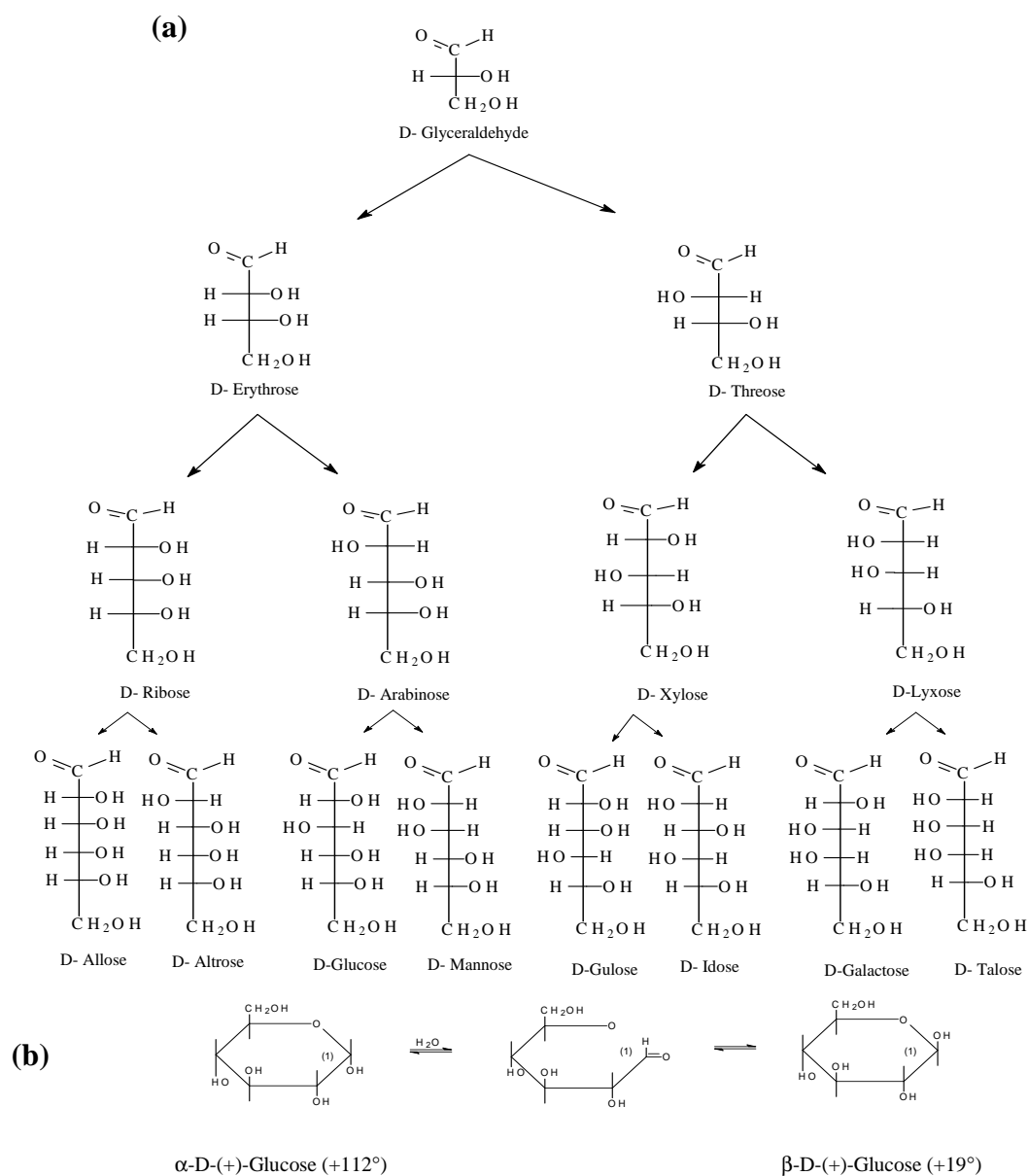


Fig. 5.15. (a) Examples of open-chain forms of monosaccharides. (b) Cyclic structures of D-(+)-glucose (mutarotation process).

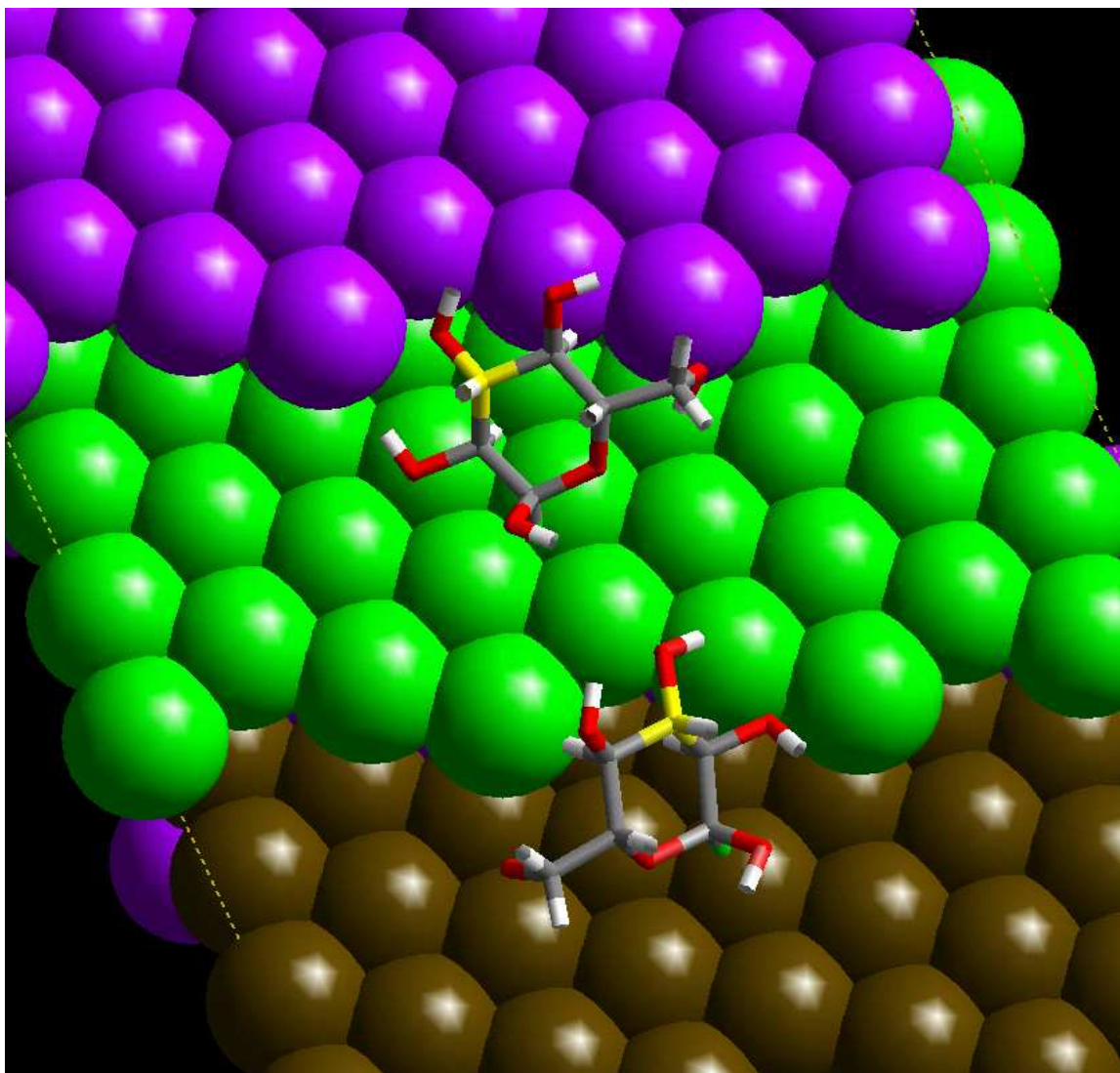


Fig. 5.16. Schematic representation showing interaction of chiral carbon centre 3 (highlighted in yellow) with a chiral Pt(643)^S surface for D-(top) and L-glucose (bottom). The hydrogen at position 1 is directed toward the (111) terrace and has been coloured green.

5.4. References

1. C. F. McFadden, P. S. Gremer, A. J. Gellman, *Langmuir*, **12** (1996) 2483.
2. G. A. Attard, C. J. Barnes, *Surfaces*, Oxford University Press, Oxford, UK., 1998, pp. 71.
3. M. A. Van Hove, G. A. Somorjai, *Surf. Sci.*, **92** (1980) 489.
4. D. S. Sholl, *Langmuir*, **14** (1996) 862.
5. A. Ahmadi, G. Attard, J. Feliu, A. Rodes, *Langmuir*, **15** (1999) 2420.
6. G. A. Attard, A. Ahmadi, J. Feliu, A. Rodes, E. Herrero, S. Blais, G. Jerkiewicz, *J. Phys. Chem.*, **B 103** (1999) 1381.
7. M. L. B. Roa, R. F. Drake, *J. Electrochem. Soc.*, **116** (1969) 334.
8. S. J. Yao, A. J. Appleby, S. K. Wolfson, Jr. *Z. Phys. Chem. N. F.* **82** (1972) 225.
9. E. Skov, *Electrochim. Acta*, **22** (1977) 313.
10. S. Ernst, J. Heitbaum, C. H. Hamman, *J. Electroanal. Chem.*, **100** (1979) 173.
11. Y. B. Vassilyev, G. A. Kharzova, N. N. Nikolaeva, *J. Electroanal. Chem.*, **196** (1985) 127.
12. L. H. Essis Yei, B. Beden, C. Lamy, *J. Electroanal. Chem.*, **246** (1988) 349.
13. G. Kokkiniois, J. M. Leger, C. Lamy, *J. Electroanal. Chem.*, **242** (1988) 221.
14. K. Popovic, A. Tripkovic, N. Markovic, R. R. Adzic, *J. Electroanal. Chem.*, **295** (1990) 79.
15. M. J. Llorca, J. M. Feliu, A. Aldaz, J. Clavilier, A. Rodes, *J. Electroanal. Chem.*, **316** (1991) 175.
16. A. Rhodes, M. J. Llorca, J. M. Feliu, J. Clavilier, *Anal. Quim. Int. Ed.* **92** (1996) 118.
17. K. D. Popovic, A. V. Tripkovic, R. R. Adzic, *J. Electroanal. Chem.* **339** (1992) 227.
18. Y. Orito, S. Imai, S. Niwa, in *Collected Papers of the 43rd Catalyst Forum, Japan*, **30**, 1978
19. R. T. Morrison, R. N. Boyd, *Organic Chemistry*, 3rd ed., Allyn and Bacon, M. A. Boston, 1973.
20. A. Rodes, K. El-Achi, M. A. Zamakhchari, J. Clavilier, *J. Electroanal. Chem.*, **284** (1990) 245.
21. J. Clavilier, K. El-Achi, A. Rodes, *Chem. Phys.*, **141** (1991) 1.
22. G. A. Attard, *Phys. Chem.*, **B 105** (2000) 3158.
23. R. T. Morrison, R. N. Boyd, *Organic Chemistry*, 3rd ed., Allyn and Bacon, M. A. Boston, 1973, pp. 1095
24. D. Watson, G. Attard, *J. Electrochimica. Acta*, **46** (2001) 3157.